

INFLUENCE OF DIFFERENT SUPPORTING STIFFNESS AND FLUID VELOCITIES ON VIBRATION CHARACTERISTIC OF HYDRAULIC PIPE

LINGXIAO QUAN^{1,2}, HONGLIANG LUO², XU DING² AND HUANHUAN BAI³

¹Key Laboratory of Advanced Forging and Stamping Technology and Science (Yanshan University)
Ministry of Education of China
No. 438, Hebei Ave., Qinhuangdao 066004, P. R. China
lingxiao@ysu.edu.cn

²Hebei Provincial Key Laboratory of Heavy Machinery Fluid Power Transmission and Control
Yanshan University
No. 438, Hebei Ave., Qinhuangdao 066004, P. R. China

³DHHI Hydraulic Equipment Plant
Dalian 116000, P. R. China

Received August 2015; accepted November 2015

ABSTRACT. *This paper was concerned with the vibration characteristic of hydraulic pipe's FSI (Fluid-Structure Interaction), and we especially analyzed the influence of different supporting stiffness and fluid velocities. At first, we had set up the FSI dynamics simulation model of single hydraulic straight pipe using ADINA (Automatic Dynamic Incremental Nonlinear Analysis). Besides, we made the numerical analysis and analyzed pipe vibration characteristic, such as the vibration mode and natural frequency with different supporting stiffness. Then we researched pipe vibration response (displacement, velocity, acceleration and stress) changing with different fluid velocities. The last but not the least, we set the aviation hydraulic pipe vibration rule with different supporting stiffness and fluid velocities, which laid the foundation of aviation hydraulic pipe vibration research.*

Keywords: Vibration characteristic, Supporting stiffness, Fluid velocity

1. Introduction. The development of large aircraft has made great achievements in China. The amount of large aircraft will be about 3000 in 2016. Consequently, it is urgent to develop the control and actuation system with electro-hydraulic power independently [1,2]. At present, the trend of large aircraft hydraulic control system is 'the bigger velocity, the higher pressure, and the higher power-weight ratio'. As is known, the current pressure system of large aircraft is 35MPa, and 42MPa is on the near future. With the increase of the system pressure, the pipe's FSI vibration magnitude and frequency become big, causing series of problems, such as aggravating unsteady fluid flow, reinforcing coupled vibration, enhancing pipe's vibration and noise, which presents a new challenge to design and optimize large aircraft hydraulic pipeline system.

Various nonlinear factors affect hydraulic pipe's FSI vibration, and the pipe constraint form determines the accuracy of the FSI vibration model. The FSI vibration mechanism is arduous to explore because of the complexity of the working condition and support constraint [3,4]. The study of pipe vibration usually focuses on pipe vibration mode, pipe stiffness and damping characteristic at home and abroad. However, the research on influence of the supporting condition changing on the pipe vibration has captured scholars' attention recently.

In 1980, Noah and Hopkins studied the pipe with one side fixed and the other side supported by displacement and torsion springs, presenting that the supporting stiffness and fluid velocity have great impact on the system instability [5]. In 2007, Chellapilla and

Simha got the critical pipe flow velocity of FSI, using Galerkin method and Fourier series [6]. In 2010, Huang et al. got the speed when the system is instable, by the Galerkin method, ignoring the Coriolis force [7]. In 2013, Huang et al. concluded the changing trend of frequency and amplitude with different supporting stiffness, considering the pipe's FSI vibration [8]. The vortex-induced vibration of a long flexible pipe conveying fluctuating flows is investigated; the results indicate that if a pipe containing fluctuating flows, the peak of vibration amplitudes is larger than that of a pipe conveying steady flow [9].

In the past, the researchers have achieved the calculation method of hydraulic piping vibration natural frequency and the factors of hydraulic piping vibration. However, the research in the past did not involve the impact of supporting stiffness and fluid velocity on hydraulic pipe vibration. So in this paper, the influence of different supporting stiffness and fluid velocities on pipe vibration was analyzed based on the FSI mathematical model of pipe. At first, the hydraulic pipe model is established. Then the hydraulic pipe vibration characteristic with different supporting stiffness is analyzed. At last, the hydraulic pipe vibration response corresponding to different inlet flow rates is concluded.

2. FSI Mathematical Dynamics Model of Hydraulic Pipe. In Figure 1, there are four support forms of hydraulic pipe. Figure 1(a) manifests cantilevers model, Figure 1(b) manifests two-side simply supported model, Figure 1(c) manifests simply supported at one side and fixed at the other side, and Figure 1(d) manifests two-side fixed model. First and foremost, the pipe axial movement must comply with none axis extension theorem, namely, pipe axial force is zero. Subsequently, the pipe axial movement should comply with the theorem that its axis is extensible when it is simply supported in either side [10].

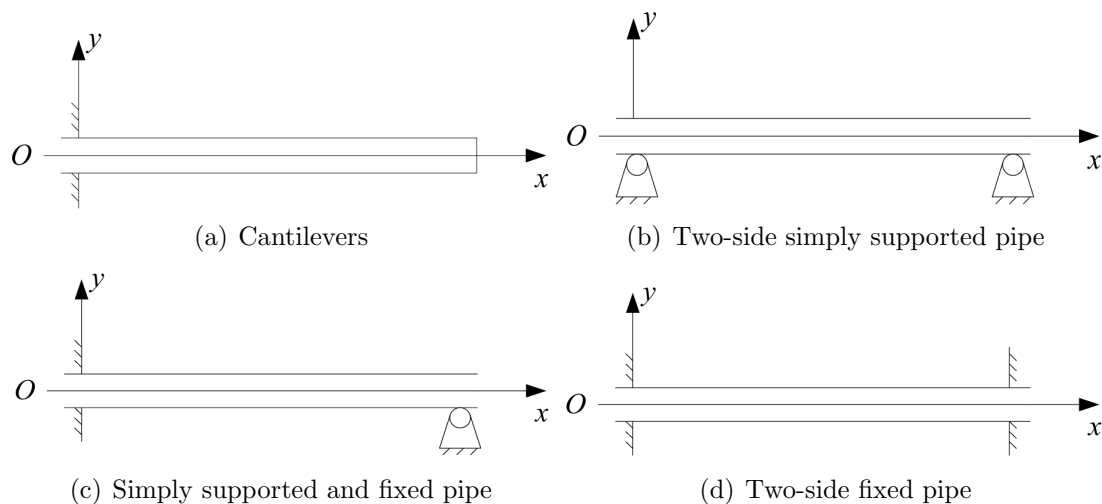


FIGURE 1. Forms of different supported pipes

Generally, Figure 2 demonstrates the hydraulic pipe and its internal fluid micro-element dynamic analysis model. Considering the influence of axial stress waves, we build the 4-equation dynamic analysis model of FSI vibration based on the extending water hammer theory. Usually, we describe the fluid mechanics equation by the continuity equation, momentum equation, and energy equation. Additionally, shear, bend and deformation are ignored.

$$\frac{\partial V_f}{\partial t} + \frac{1}{\rho_f} \frac{\partial P}{\partial z} = 0 \quad (1)$$

$$\frac{\partial V_f}{\partial z} + \left\{ \frac{1}{K_f} + \frac{2R}{E\delta} \right\} \frac{\partial P}{\partial t} - \frac{2v}{E} \frac{\partial \sigma_z}{\partial t} = 0 \quad (2)$$

$$\frac{\partial \dot{u}_z}{\partial t} - \frac{1}{\rho_p} \frac{\partial \sigma_z}{\partial z} = 0 \tag{3}$$

$$\frac{\partial \dot{u}_z}{\partial z} - \frac{1}{E} \frac{\partial \sigma_z}{\partial t} + \frac{vR}{E\delta} \frac{\partial P}{\partial t} = 0 \tag{4}$$

where, V_f is the average fluid velocity per unit length, ρ_f is the fluid density, P is the fluid pressure, z is the z -axis direction (pipe axial direction is x , and the lateral displacement is y and z directions), K_f is the bulk modulus of the fluid, σ_z is the average axial stress at the pipe cross-section, δ is thickness of pipe wall, E is Young's modulus of the pipe, v is Poisson's ratio, ρ_p is the density of the line, \dot{u}_z is the axial velocity of the pipe, R is the pipe radius, and t is time item.

Actually, the pipe's supporting state should be considered as the variable stiffness, since domestic and foreign scholars generally simulate the real state with the variable spring stiffness. Figure 3 demonstrates the three-dimensional Cartesian coordinate system. During the study, the following assumptions are made.

1. There is no coupling between axial movement and lateral movement of the pipe.
2. The wall material is uniform, isotropic and linear.

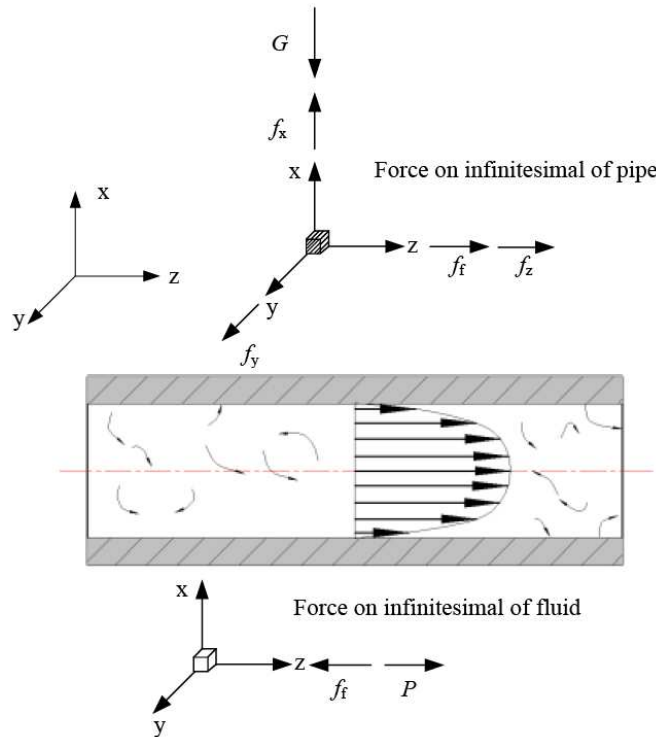


FIGURE 2. Piping and fluid micro-element model

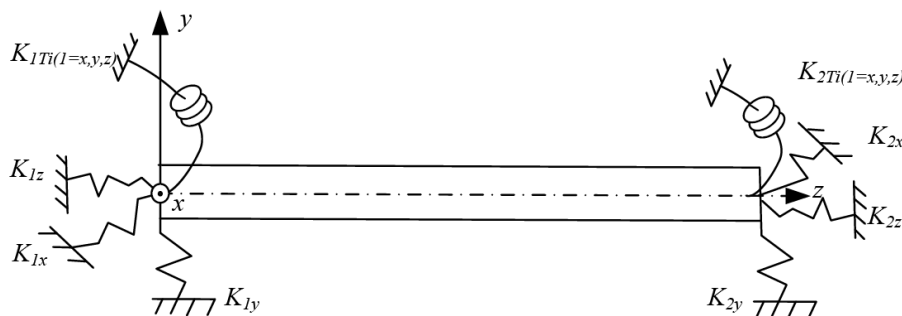


FIGURE 3. Hydraulic pipe model with six springs

3. The internal medium is compressible Newtonian fluid, and its velocity of flow is much less than the critical velocity of turbulence.

We should establish the hydraulic pipe model based on elastic supporting. In Figure 3, axial movement of the pipeline is along the z -axis direction, and two lateral movements perpendicular to the axis are along the x -axis and the y -axis directions, respectively. Pipe's three liner movements and three rotation movements at x , y and z directions are replaced by three linear springs and three torsion springs. The different supporting states can be changed by different spring stiffness values [11].

3. The Analysis of Vibration Characteristic with Different Supporting Stiffness. The finite elements software ADINA system focuses on solving nonlinear and multiple physical coupling problems [12]. It has higher solving efficiency, and better reliability. It enables to solve complex nonlinear problems well in coupling fields such as solid, flow, heat, and magnetic.

The right end of pipe uses fixed constraint, and the left uses the six-degree of freedom linear spring constraint, which can simulate the support direction and elastic stiffness values. In this way, FSI vibration characteristic can be found by the potential fluid element. Also, we can find the effect of the changing elastic supporting stiffness on the natural frequency of the fluid-filled straight pipe [13].

Setting different supporting stiffness, we can obtain first-order natural frequency curves of hydraulic pipe as Figure 4 manifests. Results indicate that the first-order natural frequency increases with the increase of supporting stiffness. When supporting stiffness is about $1 \times 10^4 \text{N/m}$, the rising rate of first-order natural frequency increases rapidly. When supporting stiffness is greater than $1 \times 10^8 \text{N/m}$, the first-order natural frequency is stable, which is almost the same as the two-side fixed. Figure 5 manifests the first-order natural frequency curves of empty and liquid pipes. Results infer that considering FSI effect, the trend of first-order natural frequency is complex with the increase of supporting stiffness. When the supporting stiffness is about $2 \times 10^3 \text{N/m}$, the vibration frequency of empty pipe is the same as that of liquid pipe, but if the supporting stiffness is smaller than $2 \times 10^3 \text{N/m}$, the vibration frequency of empty pipe is smaller than the liquid one.

Figure 6 manifests the first-order and second-order natural frequency curves of hydraulic pipe. Results suggest that the changing trends of two curves are almost the same. Figure 7 manifests the first 20-order natural frequency histogram of empty pipe when stiffness is $1 \times 10^4 \text{N/m}$, $1 \times 10^7 \text{N/m}$ and $1 \times 10^{13} \text{N/m}$. Results imply that the supporting stiffness has impact on each order vibration modal. As the stiffness increases, each order natural

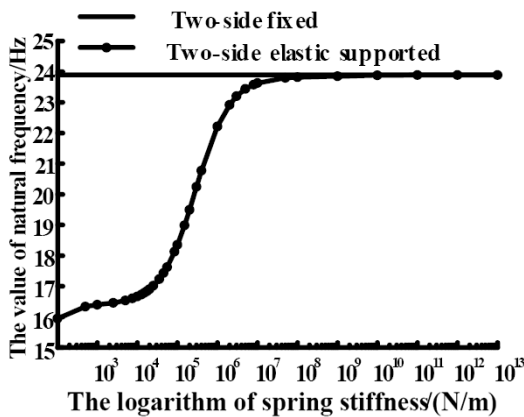


FIGURE 4. First-order natural frequency curves corresponding to different stiffness values

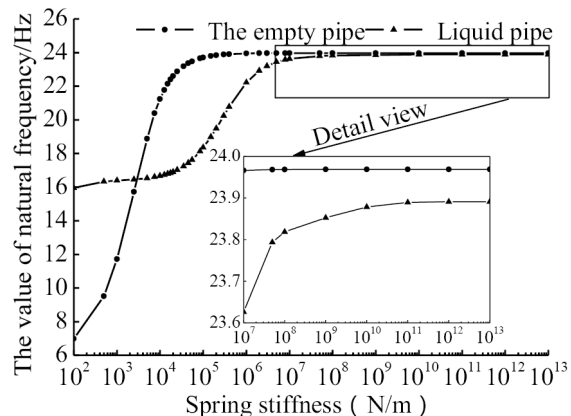


FIGURE 5. First-order natural frequency of empty and straight pipes filled with hydraulic oil

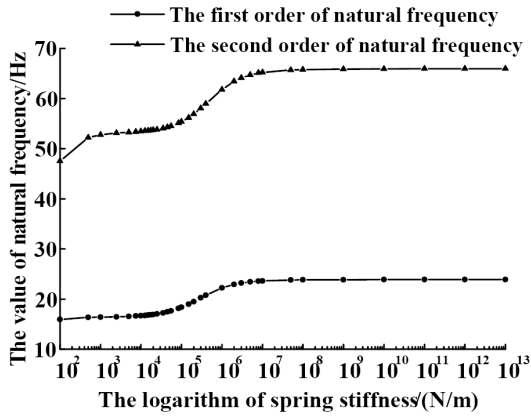


FIGURE 6. First-order and second-order natural frequency curves corresponding to different stiffness values

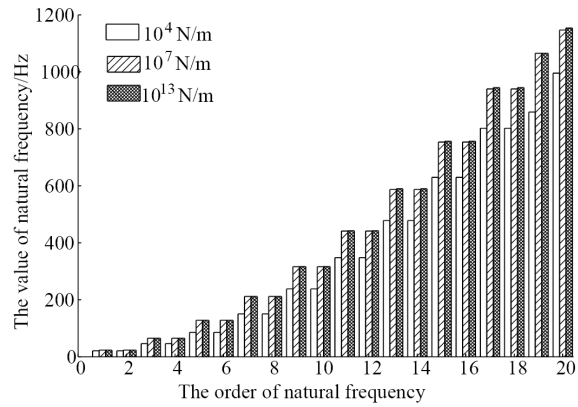


FIGURE 7. Top 20 orders natural frequencies corresponding to different stiffness values

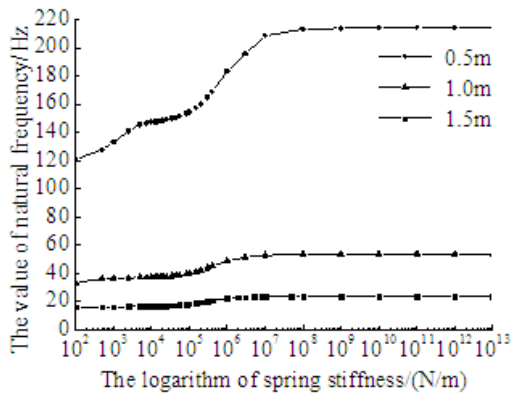


FIGURE 8. First-order natural frequency curves corresponding to different length

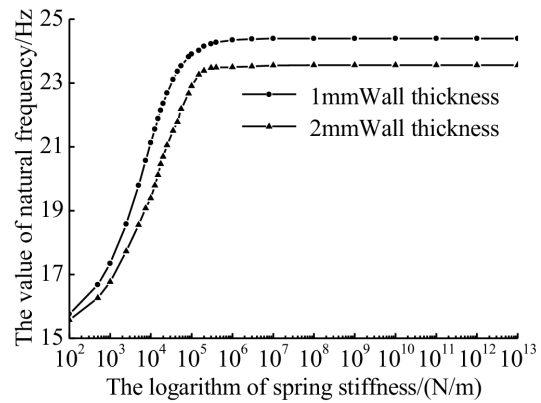


FIGURE 9. First-order natural frequency curves corresponding to different wall thickness

frequency increases, too. When the supporting stiffness value is greater than 10^7N/m , the pipe’s supporting state should be considered as fixed support.

Figure 8 manifests the first-order natural frequency curves with different pipe length. Results indicate that the first natural frequency decreases with the increasing of pipe length. Figure 9 manifests the change curves of the first-order vibration frequency with different pipe wall thickness. Results infer that the first natural frequency decreases when the thickness of the pipe adds up from 1mm to 2mm. Figure 10 manifests the first-order natural frequency curves of the liquid pipe with different outside diameters. Results suggest that the first natural frequency of the fluid pipe increases when the pipe diameter adds up from 10mm to 20mm.

4. Vibration Response Analysis on Hydraulic Pipe Corresponding to Different Inlet Flow Rates. The amplitude and frequency of flow pulsation are mainly related to piston number and swash plate angle. If swash plate angle is changed only, the pulsation amplitude of pump outlet will not change. However, the average velocity of flow will change [14].

In the first place, the following boundary condition is set.

1) The average fluid velocity of the pipe inlet is respectively set to be 2m/s, 5m/s and 10m/s.

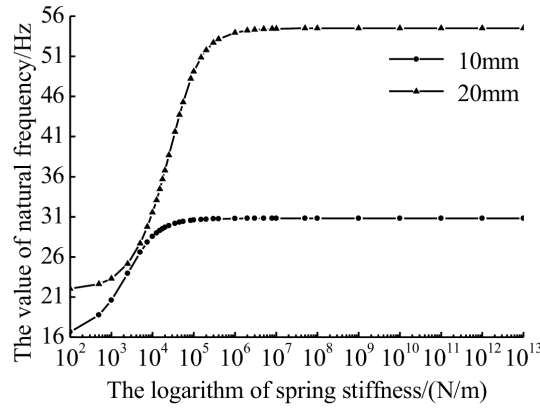


FIGURE 10. Different first-order frequency curves corresponding to different diameters

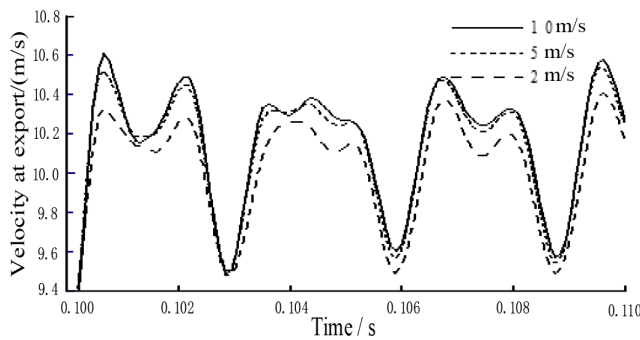


FIGURE 11. Outlet fluid velocity curves through pipe cross section corresponding to different average fluid velocities

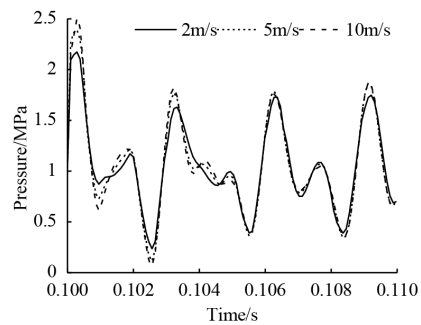


FIGURE 12. Inlet pressure corresponding to different velocities of flow

2) Supporting stiffness of hydraulic pipe bracket used in aircraft is relatively lower, so we should set the supporting stiffness to be $1 \times 10^4 \text{N/m}$.

The velocity of flow changing curve through pipe cross section is set in ADINA system. The slope curve demonstrates that the velocity increases from 0m/s to the valley of velocity fluctuation within 0.1 second. The sine stage manifests that the fluid velocity pulsation frequency is 350Hz. The last but not the least, the outcome documents of the fluid and pipe are introduced, and results such as fluid entrance velocity, pressure, intermediate point acceleration, effective stress, reaction force of spring side and fixed end, are corresponding to different average fluid velocities [15].

Adjusting the inlet velocity with speed control valve, we can obtain numerous vibration response on hydraulic pipe in the case of various inlet velocities. Figure 11 manifests the outlet fluid velocity curves through pipe corresponding to different average fluid velocities. Results imply that the velocity amplitude through pipe outlet goes up with the increase of average velocity of flow. Figure 12 manifests the inlet pressure corresponding to different average velocities of flow. Results indicate that when the average entrance velocity increases, the pressure fluctuation amplitude will increase, but after two cycles, it has the same amplitude.

Figure 13 manifests the vibration acceleration amplitude curves of the intermediate point on pipe outside surface corresponding to different average velocities of flow. Result infers that acceleration amplitude increases with the increase of the average velocity of flow. Vibration acceleration presents high frequency fluctuation, and as the vibration of transmission, the acceleration value also presents the sine wave. Figure 14 manifests

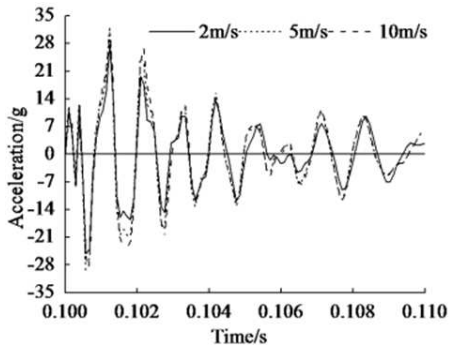


FIGURE 13. The vibration acceleration amplitude curves corresponding to different velocities of flow

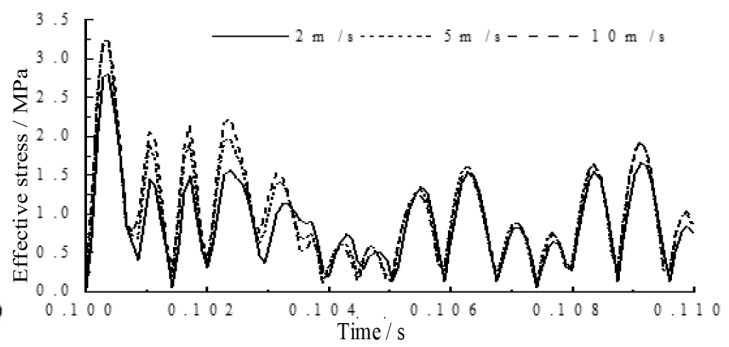


FIGURE 14. The effective stress curves corresponding to different velocities of flow

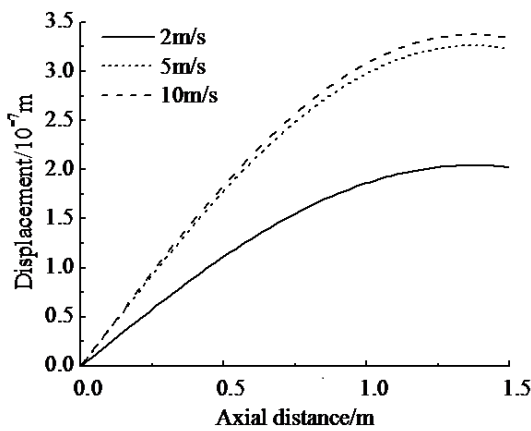


FIGURE 15. Displacement corresponding to different velocities of flow

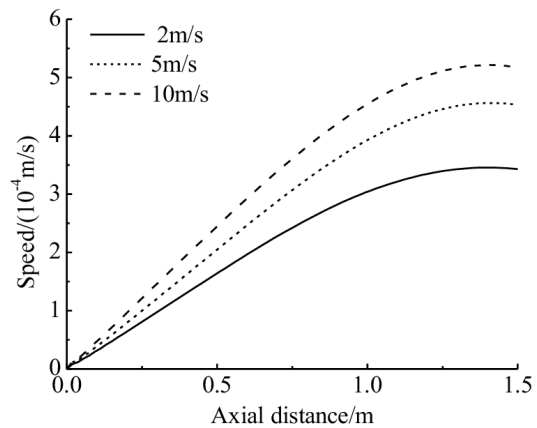


FIGURE 16. Velocity corresponding to different velocities of flow

the effective stress curves of pipe's intermediate point corresponding to different average velocities of flow. Result suggests that effective stress increases with the increase of the average velocity of flow. And effective stress presents high frequency vibration.

Figure 15, Figure 16 and Figure 17 manifest the displacement, speed and acceleration along the pipe axis curves on the pipe surface corresponding to different average velocities, respectively. Results imply that from the fixed end to the elastic end, the displacement, velocity and acceleration increase at first and then decrease slowly. When the average velocity at the entrance increases, they will increase.

Figure 18 manifests the effective stress distribution curves along the line axis on the pipe surface corresponding to different average velocities of flow. Results indicate that from the fixed end to the elastic end, the effective stress shocks at the fixed end, and then decreases along the pipe axis, but it will increase at the elastic end. When the average velocity at the entrance increases, the effective stress will increase. Figure 19 manifests the reaction force amplitude curves of the pipe's fixed end corresponding to different average velocities of flow. Results infer that their vibration frequency is equal to the acceleration frequency of the pipe intermediate point. When the average velocity at the entrance increases, the reaction force will increase. Figure 20 manifests the reaction force curves of the pipe's elastic supported end corresponding to different average velocities of flow. Results suggest that when it is negative, it indicates that the axial linear spring is on the compression state. The minus only represents the direction of force, and does not

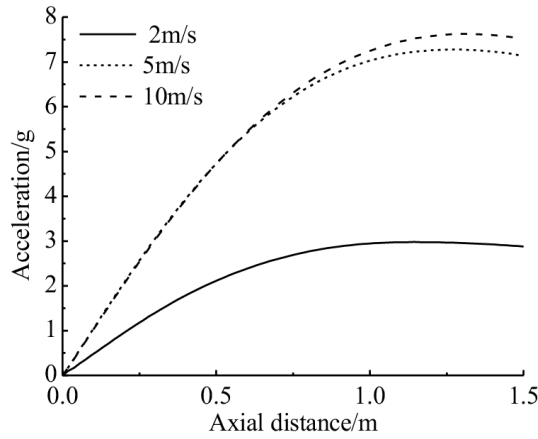


FIGURE 17. Acceleration corresponding to different velocities of flow

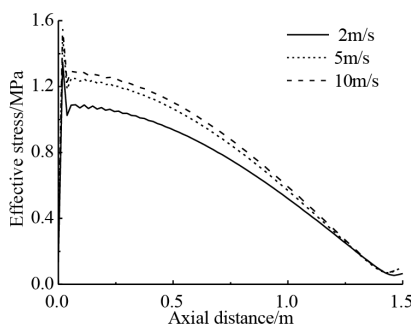


FIGURE 18. Effective stress corresponding to different velocities of flow

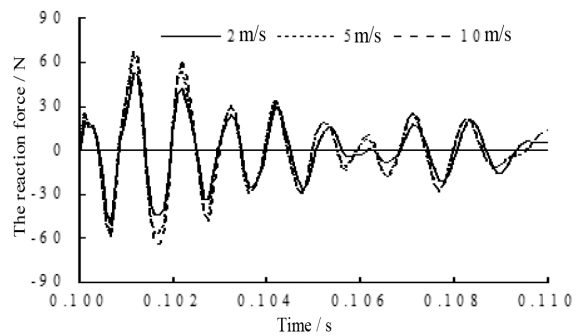


FIGURE 19. Reaction force amplitude curves of the pipe's fixed end corresponding to different velocities of flow

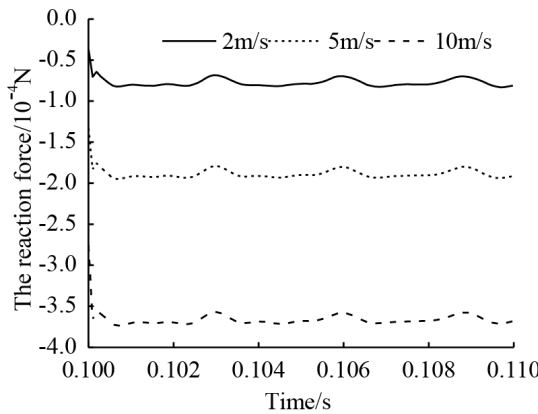


FIGURE 20. Reaction force amplitude curves of the pipe's elastic supported end corresponding to different velocities of flow

represent the numerical size. So when the average velocity increases, the reaction force will increase.

5. **Conclusion.** The changing of pipe's supporting stiffness and the average fluid velocity of pipe has great impact on the response characteristic. The following conclusions can be drawn through the above analysis.

(1) As pipe's supporting stiffness increases, every natural frequency increases. If it is greater than 10^7N/m , the pipe support basically should belong to clamped one.

(2) As the pipe length increases, the first natural frequency decreases. As the pipe thickness increases, the first natural frequency decreases. With an increase of pipe diameter, the first natural frequency increases.

(3) When the average velocity at the entrance increases, outlet velocity of flow, pressure, intermediate point acceleration, effective stress, reaction force of spring side and fixed end will increase, too.

(4) From the fixed end to the elastic end, the displacement, velocity and acceleration increase at first and then decrease slowly. However, the effective stress shocks at the fixed end, and then decreases along the pipe axis, and it will increase at the elastic end.

The results of the study can lay the foundation of aviation hydraulic pipeline vibration control and optimization. The main work of my research in the future will concentrate on how to control the vibration of the aviation hydraulic pipeline.

Acknowledgment. Research work in this paper is supported by the National Basic Research Program of China (973 Program, No. 2014CB046405), National Natural Science Foundation (No. 51375423) and the State Key Laboratory of Fluid Power Transmission and Control (No. GZKF-201309).

REFERENCES

- [1] J. Wen, Let Chinese large aircraft flying in the blue sky, *Defence Industry Conversion in China*, vol.3, pp.16-17, 2010.
- [2] C. Yang, M. Yi and B. Li, Coupled vibration of piping system conveying unsteady flow, *China Mechanical Engineering*, vol.19, no.4, pp.406-410, 2008.
- [3] K. N. Karagiozis, M. P. Païdoussis and M. Amabili, Effect of geometry on the stability of cylindrical clamped shells subjected to internal fluid flow, *Computers and Structures*, vol.85, pp.645-659, 2007.
- [4] M. Amabili, K. N. Karagiozis and M. P. Païdoussis, Effect of geometric imperfections on non-linear stability of circular cylindrical shells conveying fluid, *International Journal of Non-Linear Mechanics*, vol.44, pp.276-289, 2009.
- [5] S. T. Noah and G. R. Hopkins, Dynamic stability of elastically supported pipes conveying pulsating fluid, *Journal of Sound and Vibration*, vol.71, pp.109-116, 1980.
- [6] K. R. Chellapilla and H. S. Simha, Critical velocity of fluid-conveying pipes resting on two-parameter foundation, *Journal of Sound and Vibration*, vol.302, pp.387-397, 2007.
- [7] Y. M. Huang, Y. S. Liu, B. H. Li et al., Natural frequency analysis of fluid conveying pipeline with different boundary conditions, *Nuclear Engineering and Design*, vol.240, no.3, pp.461-467, 2010.
- [8] Y. Huang, S. Ge and W. Wu, Effect of different supporting rigidities on dynamic characteristics integrity of a pipeline conveying fluid, *Journal of Vibration and Shock*, vol.32, no.7, pp.165-168, 2013.
- [9] H. L. Dai, L. Wang, Q. Qian et al., Vortex-induced vibrations of pipes conveying pulsating fluid, *Ocean Engineering*, vol.77, pp.12-22, 2014.
- [10] J. H. You and K. Inaba, Fluid-structure interaction in water-filled thin pipes of anisotropic composite materials, *Journal of Fluids and Structures*, vol.36, pp.162-173, 2013.
- [11] J. Jin, Z. Qin and D. Li, A simplified model for a slender flexible cylinder subjected to axial flow and its dynamic characteristics, *Journal of Vibration Engineering*, vol.24, no.1, pp.27-30, 2011.
- [12] W. J. Guo, T. Y. Li, X. Zhu et al., Vibrational frequencies calculation of fluid conveying pipes based on fluid-structure coupling and acoustic-structure coupling models, *Applied Mechanics and Materials*, vol.574, pp.41-47, 2014.
- [13] W. Feng, L. Song and G. Xiao, Coupling analysis of fluid-structure interaction in pressure pipes based on ADINA, *Engineering Journal of Wuhan University*, vol.42, pp.264-267, 2009.
- [14] J. Jin, X. Yang and G. Zou, Stability and critical fluid velocity of supported pipes conveying fluid, *Chinese Journal of Mechanical Engineering*, vol.11, pp.131-136, 2006.
- [15] D. J. Montoya-Hernández, A. O. Vázquez-Hernández, R. Cuamatzi et al., Natural frequency analysis of a marine riser considering multiphase internal flow behavior, *Ocean Engineering*, vol.92, pp.103-113, 2014.